

# Solving the Liouvillian Gap with Artificial Neural Networks

Dong Yuan,<sup>1,2,\*</sup> Heran Wang,<sup>2,3,\*</sup> Zhong Wang,<sup>3,†</sup> and Dong-Ling Deng<sup>1,4,‡</sup>

<sup>1</sup>Center for Quantum Information, IIS, Tsinghua University, Beijing 100084, People's Republic of China

<sup>2</sup>Department of Physics, Tsinghua University, Beijing 100084, People's Republic of China

<sup>3</sup>Institute for Advanced Study, Tsinghua University, Beijing 100084, People's Republic of China

<sup>4</sup>Shanghai Qi Zhi Institute, 41th Floor, AI Tower, No. 701 Yunjin Road, Xuhui District, Shanghai 200232, China

We propose a machine-learning inspired variational method to obtain the Liouvillian gap, which plays a crucial role in characterizing the relaxation time and dissipative phase transitions of open quantum systems. By using the “spin bi-base mapping”, we map the density matrix to a pure restricted-Boltzmann-machine (RBM) state and transform the Liouvillian superoperator to a rank-two non-Hermitian operator. The Liouvillian gap can be obtained by a variational real-time evolution algorithm under this non-Hermitian operator. We apply our method to the dissipative Heisenberg model in both one and two dimensions. For the isotropic case, we find that the Liouvillian gap can be analytically obtained and in one dimension even the whole Liouvillian spectrum can be exactly solved using the Bethe ansatz method. By comparing our numerical results with their analytical counterparts, we show that the Liouvillian gap could be accessed by the RBM approach efficiently to a desirable accuracy, regardless of the dimensionality and entanglement properties.

Studies of open quantum systems have attracted tremendous attentions across a wide variety of fields [1, 2], ranging from condensed matter physics to quantum simulation [3] and quantum information processing [4]. Within the Markovian approximation, the dynamics of an open quantum system is governed by the Lindblad master equation. Relevant to this equation, a fundamental quantity that characterizes the relaxation time and dissipative phase transitions of open quantum systems is the so-called Liouvillian gap, defined as the gap between the first and second largest real parts of the eigenspectrum of the Liouvillian superoperator. For quantum many-body systems, obtaining the Liouvillian gap poses a notorious challenge for both analytical and numerical approaches, owing to the exponential scaling of the Hilbert space dimension with the system size. Despite a few pronounced solvable examples [5–13], a flexible and scalable numerical approach to compute the Liouvillian gap is still lacking hitherto. Here, we add this crucial yet missing block by introducing a generic machine-learning inspired variational method, with a focus on the restricted-Boltzmann-machine (RBM) architecture (see Fig. 1 for a pictorial illustration).

From the numerical computation point of view, computing the Liouvillian gap is a formidable task in general. In fact, it has been rigorously proved that the general spectral gap problem is undecidable even for closed quantum systems [14–16]: there exists *no* algorithm to determine whether an arbitrary Hamiltonian is gapped or not. Computing the Liouvillian gap is even harder in general. Fortunately, physical Hamiltonians or Liouvillians of practical interest often bear special structures, which may enable them to circumvent the undecidability and make their spectral gaps accessible by certain numerical methods. In particular, for solving Lindblad master equations to obtain the dynamics and non-equilibrium steady states of open quantum systems, a number of notable algorithms have been proposed, including matrix-product state and tensor network approaches [17–23], corner-space renormalization [24, 25], cluster mean-field [26], and quantum Monte Carlo [27–29]. More recently, machine learn-

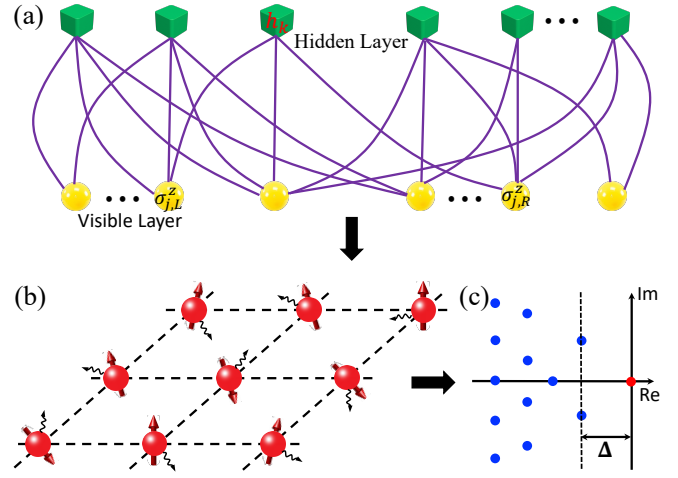


FIG. 1. A sketch of the essential idea for accessing the Liouvillian gap with artificial neural networks. (a) The restricted Boltzmann machine (RBM) representation of quantum many-body density matrices under the “spin bi-base mapping”. (b) The dissipative spin-1/2 XYZ model defined on a 2D square lattice. Each spin interacts with its nearest neighboring spins and is subject to a dissipation process into the  $|\sigma^z = -1\rangle$  state [see Eq. (7)]. (c) A pictorial sketch of the Liouvillian spectrum for the dissipative XYZ model. The red dot corresponds to the non-equilibrium steady state with zero Liouvillian eigenvalue, whereas the blue dots on the vertical dotted line correspond to the first decay modes. The Liouvillian gap  $\Delta$  is defined as the real part of the spectral gap between the eigenvalues corresponding to the first decay modes and the steady state.

ing [30] approaches based on artificial neural networks have also been invoked to tackle this problem [31–34]. The essential idea is to use neural network quantum states [35–39], especially the RBM states [35, 36], to serve as ansatz density matrices for open quantum systems and adopt the stochastic reconfiguration (SR) method [40] to obtain their dynamics and steady states by solving the master equation variationally. Owing to the structure flexibility and long-range connections of neural networks, such approaches admit the striking merit

of generic applicability to high dimensional systems with even volume-law entanglement [41].

In this paper, we introduce a variational method based on the RBM representation to compute the Liouvillian gap. We use the "spin bi-base mapping" to map the density matrix to a pure state that is conveniently represented by RBMs. Under this mapping, the Liouvillian superoperator reduces to a rank-two non-Hermitian operator and the Liouvillian gap can be computed by the variational SR algorithm [40]. To demonstrate and benchmark the accuracy and efficiency, we apply our method to the dissipative XYZ (also known as Heisenberg) models in both one and two dimensions (2D). We find that for the isotropic case (the dissipative XXZ model), the Liouvillian gap is always equal to half of the dissipation rate, independent of the coupling strengths, system sizes, and lattice geometry. Inspired by this observation, we show that for the dissipative XXZ model the Liouvillian gap is indeed exactly solvable, although the Liouvillian spectrum is *not* solvable in general. In 1D, we show that the whole Liouvillian spectrum can be exactly solved using the Bethe ansatz method. These analytic results may be of independent interest. For the anisotropic case, we compare our RBM results with the results from exact diagonalization (ED) and find that they match within a desirable accuracy.

*The Liouvillian gap and RBM approach.*—Under the Markovian approximation, the dynamics of an open quantum system is governed by the following Lindblad master equation [1, 2]:

$$\frac{d\rho}{dt} = -i[H, \rho] + \sum_{\mu} (2L_{\mu}\rho L_{\mu}^{\dagger} - \{L_{\mu}^{\dagger}L_{\mu}, \rho\}) \equiv \mathcal{L}\rho, \quad (1)$$

where  $\rho$  denotes the density matrix of the system,  $H$  is the Hamiltonian governing the unitary part of the dynamics,  $L_{\mu}$  are the jump operators describing the dissipative process, the curly bracket represents the anticommutator, and  $\mathcal{L}$  is the Liouvillian superoperator. In general, the index  $\mu$  runs over all dissipation channels. For simplicity and concreteness, here we mainly focus on the case where each lattice site has only one dissipation channel and  $\mu$  just labels the lattice site. The generalization to the cases with multiple dissipation channels is straightforward.

The full spectrum of the Liouvillian superoperator  $\mathcal{L}$  can be determined by solving the eigenequation:  $\mathcal{L}\rho_k = \lambda_k\rho_k$ , where  $\lambda_k$  is the eigenvalue and  $\rho_k$  denotes its corresponding eigenmatrix. Unlike the case of closed quantum systems, the eigenvalues of  $\mathcal{L}$  are usually complex and their corresponding eigenmatrices are not necessarily physical (i.e., being Hermitian, trace-one, and semi-positive definite). Moreover, it can be proved [1] that  $\text{Re}(\lambda_k) \leq 0$  for all  $k$ . For convenience, we sort the eigenvalues by their real parts in decreasing order [ $\text{Re}(\lambda_0) \geq \text{Re}(\lambda_1) \geq \dots$ ] with the steady state corresponding to  $\lambda_0 = 0$  (for simplicity, we only focus on the case that the steady state is unique and  $\lambda_0$  has no degeneracy). With this convention, the Liouvillian gap is defined as

$$\Delta = -\text{Re}(\lambda_1). \quad (2)$$

The Liouvillian gap is a central and fundamental physical quantity in studying open quantum systems. It determines the relaxation time from an arbitrary initial state to the steady state and plays an crucial role in characterizing dissipative phase transitions [42, 43] and the exotic chiral damping phenomenon [44]. Yet, for quantum many-body systems the dimension of the Liouville space scales double exponentially with the system size, rendering the computation of Liouvillian gap notably challenging.

Here, we propose a neural network approach based on RBMs to tackle this problem. To this end, we first employ a spin bi-base mapping, which is also called the Choi-Jamiołkowski isomorphism [18, 23], to map a density matrix to a vector in the computational bases:

$$\rho = \sum_{m,n} \rho_{mn} |m\rangle\langle n| \Leftrightarrow \tilde{\rho} = \sum_{m,n} \rho_{mn} |m\rangle \otimes |n\rangle. \quad (3)$$

Under this mapping, the Liouvillian superoperator  $\mathcal{L}$ , originally a rank-four tensor, reduces to a rank-two operator  $\tilde{\mathcal{L}} = -iH \otimes I + iI \otimes H^T + \sum_{\mu} (2L_{\mu} \otimes L_{\mu}^* - L_{\mu}^{\dagger} L_{\mu} \otimes I - I \otimes L_{\mu}^T L_{\mu}^*)$ , where  $I$  denotes the identity matrix and  $T$  means the matrix transpose. We consider an open quantum system with  $N$  qubits and use an RBM to describe  $\tilde{\rho}$  with [35]

$$(\rho_{\text{RBM}})_{mn} = \exp \left[ \sum_{j=1}^N (a_j \sigma_{j,R}^z + b_j \sigma_{j,L}^z) \right] \prod_{k=1}^M X_k, \quad (4)$$

where  $\sigma_{j,R(L)}^z = \pm 1$  denotes the visible neurons responsible for the  $|m\rangle = |\sigma_{1,R}^z, \dots, \sigma_{N,R}^z\rangle$  ( $|n\rangle = |\sigma_{1,L}^z, \dots, \sigma_{N,L}^z\rangle$ ) part of  $\tilde{\rho}$ ,  $M$  is the number of hidden neurons, and  $X_k = \cosh \left( c_k + \sum_j W_{k,j}^R \sigma_{j,R}^z + \sum_j W_{k,j}^L \sigma_{j,L}^z \right)$ . Here,  $\{a_j, b_j, c_k\}$  are on-site weight parameters, and  $\{W_{k,j}^R, W_{k,j}^L\}$  are connection parameters between visible and hidden neurons. We note that the matrix  $\rho$  corresponding to  $\tilde{\rho}$  may *not* be physical, in contrast to the representations of density matrices introduced in Ref. [31–34, 36]. This is not a problem for our purpose because here we mainly focus on the eigenmatrices of  $\mathcal{L}$ , which are not physical in general.

Given the RBM parametrization of  $\tilde{\rho}$ , we can now recast the problem of computing the Liouvillian gap as a variational optimization problem in a subspace orthogonal to the steady state  $\rho_0$ . Yet, the subtraction of  $\rho_0$  is tricky. Analogous to the closed system case, one may regard the first decay modes as the first "excited states" of  $\mathcal{L}$  and then the Liouvillian gap is just the "first excited energy". Consequently, a possible way to obtain the Liouvillian gap is by first computing the steady state of  $\mathcal{L}$  and then appropriately extending the protocols for calculating the excited states of closed systems [46, 47] to open systems. This approach is straightforward, yet technically cumbersome. By noticing the fact that  $\text{Tr}(\mathcal{L}\rho_k) = 0 = \lambda_k \text{Tr}(\rho_k)$  and hence  $\text{Tr}(\rho_k) = 0$  for all  $\lambda_k \neq 0$ , a much simpler approach is to construct a new variational matrix  $\rho'$  with vanishing trace

$$\rho' = \alpha \rho'_0 + \rho_{\text{RBM}}, \quad (5)$$

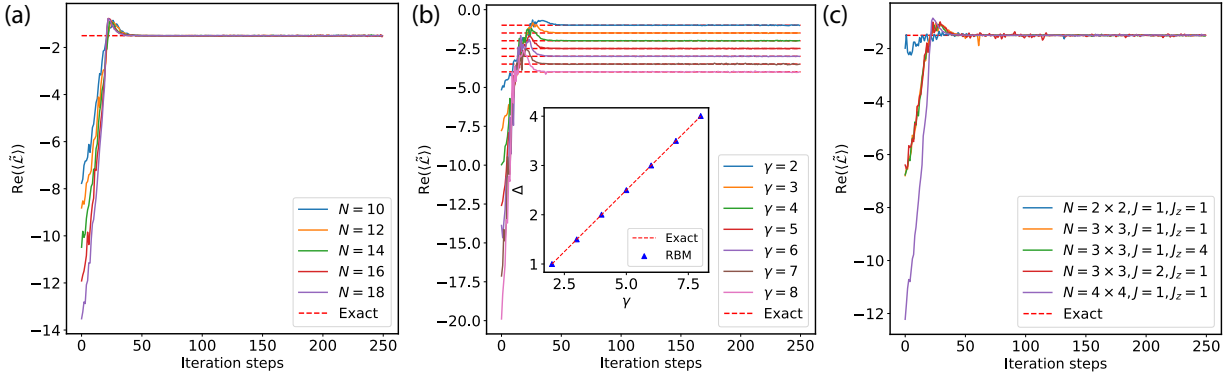


FIG. 2. Numerical results for the dissipative XXZ model in one [(a) and (b)] and two [(c)] dimensions. (a) The real part of the expectation value  $\text{Re}(\langle\tilde{\mathcal{L}}\rangle) = \text{Re}(\langle\rho'|\tilde{\mathcal{L}}|\rho'\rangle/\langle\rho'|\rho'\rangle)$  as a function of the iteration steps for different lattice sizes  $N$ . The parameters are chosen as  $J_x = J_y = 1$ ,  $J_z = 2$ , and  $\gamma = 3$ . The red dashed horizontal line indicates the exact value of the Liouvillian gap  $\Delta$  obtained by exact diagonalization, which can also be derived analytically (see the main text). (b)  $\text{Re}(\langle\tilde{\mathcal{L}}\rangle)$  as a function of iteration steps for different dissipation rates. Here,  $J_x = J_y = 1$ ,  $J_z = 2$ , and the lattice size is fixed to be  $N = 10$ . The inset shows the linear dependence of the Liouvillian gap obtained by the RBM method on the dissipation rate  $\gamma$ . (c) Numerical results for 2D dissipative XXZ model with varying lattice sizes and coupling strengths. Here, we set  $\gamma = 3$  and show  $\text{Re}(\langle\tilde{\mathcal{L}}\rangle)$  as a function of iteration steps. All the ancillary  $\rho'_0$  used here correspond to the bi-base state with all spins pointing down. More details on these numerical results are shown in the Supplemental Material [45].

where  $\alpha = -\frac{\text{Tr}(\rho_{\text{RBM}})}{\text{Tr}(\rho'_0)}$ ,  $\rho'_0$  is a density matrix with nonzero trace which is not necessary the true steady state, and  $\rho_{\text{RBM}}$  is an RBM ansatz state as defined in Eq. (4). Since  $\text{Tr}(\rho') = 0$ ,  $\rho'$  lives in the subspace orthogonal to  $\rho_0$ . We adapt the SR method [40] to generate the real time evolution of  $\rho'$  (see the Supplemental Material [45] for details). Unlike the case for closed systems,  $\tilde{\mathcal{L}}$  is not Hermitian and its right eigenvectors are not orthogonal in general. This non-Hermiticity makes the problem more complicated. We consider three different cases based on the properties of the first decay modes: (i) there is only one first decay mode, then  $\rho' \rightarrow \rho_1$  after long enough real-time evolution and the Liouvillian gap can be obtained by  $\Delta = -\text{Re}(\langle\rho'|\mathcal{L}|\rho'\rangle/\langle\rho'|\rho'\rangle)$ ; (ii) there are multiple first decay modes but they are orthogonal to each other, then  $\rho'$  will converge to a superposition of these decay modes and  $\Delta$  can still be obtained in the same way as in the first case; (iii) there exist multiple first decay modes [denoted as  $\rho_1^{(1)}, \rho_1^{(2)}, \rho_1^{(3)}, \dots$ ] which are not orthogonal. In this case,  $\rho'$  will converge to a superposition of these decay modes:

$$\rho' \rightarrow a_1\rho_1^{(1)} + a_2\rho_1^{(2)} + a_3\rho_1^{(3)} + \dots, \quad (6)$$

where  $a_1, a_2, a_3, \dots$  are coefficients whose values depend on the initialization of  $\rho'$ . Due to the non-orthogonality,  $\langle\rho_1^{(i)}|\mathcal{L}|\rho_1^{(j)}\rangle \neq 0$  for  $i \neq j$  and  $\Delta \neq -\text{Re}(\langle\rho'|\mathcal{L}|\rho'\rangle/\langle\rho'|\rho'\rangle)$  at this stage in general. To overcome this problem, we should add another imaginary time evolution for  $\rho'$  under  $i\mathcal{L}$  with a smaller learning rate so that it converges further to the first decay mode with the minimal imaginary part. After this modification,  $\Delta$  can be obtained again by computing  $-\text{Re}(\langle\rho'|\mathcal{L}|\rho'\rangle/\langle\rho'|\rho'\rangle)$  [45].

We stress the fact that the non-Hermiticity of  $\mathcal{L}$  makes the computation of the Liouvillian gap much subtler than computing the energy gap for a Hermitian Hamiltonian, as discussed above. However, the computational complexity of our

RBM approach does not increase too much and is still favorable [45]. In the following, we benchmark the effectiveness and accuracy of this approach by applying it to the dissipative XYZ models in both one and two dimensions.

*Concrete examples.*—We consider the dissipative spin-1/2 XYZ model, where each spin has a Heisenberg type interaction with its nearest neighboring spins and is subject to a dissipation process into the  $|S^z = -1/2\rangle$  state. The quantum master equation and the Hamiltonian read ( $\hbar = 1$ )

$$\frac{d\rho}{dt} = -i[H, \rho] + \frac{\gamma}{2} \sum_j [2S_j^- \rho S_j^+ - \{S_j^+ S_j^-, \rho\}], \quad (7)$$

$$H = \sum_{\langle j,k \rangle} (J_x S_j^x S_k^x + J_y S_j^y S_k^y + J_z S_j^z S_k^z), \quad (8)$$

where  $S^\mu = \frac{1}{2}\sigma^\mu$  with  $\sigma^\mu$  being the Pauli matrix ( $\mu = x, y, z$ ),  $J_\mu$  denotes the coupling constant between nearest neighboring spins,  $S^\pm = S^x \pm iS^y$ , and  $\gamma$  is the dissipation rate. The dynamics and steady state properties of this dissipative XYZ model have already been widely studied [26, 29, 31, 33, 48–51]. In particular, in 2D it exhibits a dissipative phase transition between a paramagnetic and a ferromagnetic phase [26, 29, 48–51], which originates from the competition between the unitary evolution and the incoherent dynamics. Different from the previous works that mainly focus on dynamics or steady state properties, here we focus on the computation of the Liouvillian gap instead.

We apply the introduced RBM approach to compute the Liouvillian gap for the dissipative XYZ model in both one and two dimensions. For the isotropic case  $J_x = J_y = J$ , the XYZ model reduces to the XXZ model and our numerical results are shown in Fig. 2. From this figure, it is evident that the real part of the expectation value  $\text{Re}(\langle\tilde{\mathcal{L}}\rangle) = \text{Re}(\langle\rho'|\tilde{\mathcal{L}}|\rho'\rangle/\langle\rho'|\rho'\rangle)$  converges quickly to the exact value of

the Liouvillian gap, validating the effectiveness of the RBM method. To measure the accuracy, we define the relative error  $\epsilon_{\text{rel}} = |(\Delta_{\text{RBM}} - \Delta_{\text{Ex}})/\Delta_{\text{Ex}}|$  and find that  $\epsilon_{\text{rel}} \approx 10^{-2}$  after around 50 iteration steps for all the scenarios shown in Fig. 2. We mention that the accuracy can be systematically improved by increasing the number of hidden neurons or the length of the Markov chain used in the SR algorithm [45].

An interesting observation from our RBM results shown in Fig. 2 is that for the dissipative XXZ model, the Liouvillian gap is always equal to half of the dissipation rate  $\Delta = \gamma/2$ , independent of the coupling strengths  $J$  and  $J_z$ , system size, boundary condition, and the model dimensionality. This inspired us to suspect that the Liouvillian gap is exactly solvable owing to special structures of the dissipative XXZ model. Indeed, we find that  $\Delta$  can be analytically derived as below. After the spin bi-base mapping, the Liouvillian superoperator  $\tilde{\mathcal{L}}$  for the dissipative XXZ model is mapped to:

$$\begin{aligned} \tilde{\mathcal{L}} = & -i \sum_{\langle i,j \rangle} [J_z (S_{i,R}^z S_{j,R}^z - S_{i,L}^z S_{j,L}^z)] \\ & + \frac{1}{2} J (S_{i,R}^+ S_{j,R}^- + S_{i,R}^- S_{j,R}^+ - S_{i,L}^+ S_{j,L}^- - S_{i,L}^- S_{j,L}^+) \\ & + \frac{\gamma}{2} \sum_i (2S_{i,R}^- S_{i,L}^- - S_{i,R}^z - S_{i,L}^z - 1). \end{aligned} \quad (9)$$

One may regard  $\tilde{\mathcal{L}}$  as a non-Hermitian Hamiltonian for two copies of the original dissipative system, with one copy corresponding to the right ket (the  $|m\rangle$  part) and the other copy corresponding to the left bra (the  $|n\rangle$  part) in Eq. (3). We then rearrange the terms in  $\tilde{\mathcal{L}}$  accordingly:

$$\tilde{\mathcal{L}} = H_R + H_L + \gamma \sum_i D_i, \quad (10)$$

where  $D_i = S_{i,R}^- S_{i,L}^-$  describes the couplings between the left and right spins, and  $H_R = -i \sum_{\langle i,j \rangle} [J (S_{i,R}^+ S_{j,R}^- + S_{i,R}^- S_{j,R}^+) + J_z S_{i,R}^z S_{j,R}^z] - \frac{\gamma}{2} \sum_i (S_{i,R}^z + \frac{1}{2})$  and  $H_L = i \sum_{\langle i,j \rangle} [J (S_{i,L}^+ S_{j,L}^- + S_{i,L}^- S_{j,L}^+) + J_z S_{i,L}^z S_{j,L}^z] - \frac{\gamma}{2} \sum_i (S_{i,L}^z + \frac{1}{2})$  denotes the Hamiltonians for the right and left subsystems, respectively. It is easy to observe that  $[H_L, H_R] = 0$  since they belong to different subsystems, and both  $H_L$  and  $H_R$  have a  $U(1)$  symmetry, namely their total  $S^z$  is conserved respectively. Consequently,  $\tilde{\mathcal{L}}' = H_R + H_L$  can be block-diagonalized with each block maintaining a fixed total  $S^z$ . Following Ref. [52], in the bases where  $\tilde{\mathcal{L}}'$  is block-diagonal, each term  $D_i$  is just an upper triangular matrix with vanishing diagonal terms, thus adding these terms will only alter the eigenstates but *not* the eigenvalues of  $\tilde{\mathcal{L}}'$ . As a result, the eigenspectrum of  $\tilde{\mathcal{L}}$  is exactly the same as  $\tilde{\mathcal{L}}'$  [45]. In addition, it is easy to observe that the steady state of  $\mathcal{L}$  is the state with all spins pointing down due to the dissipation process. Noting that  $\tilde{\mathcal{L}}'$  contains only imaginary XXZ interactions and a magnetic field with strength  $\frac{\gamma}{2}$ , hence the real part of the spectrum of  $\tilde{\mathcal{L}}$  is just  $-\frac{\gamma}{2}m$ , where  $m$  denotes the number of ‘‘magnons’’ created from the steady state (the number of spins flipped from down to up). As a result, the desired Liouvillian

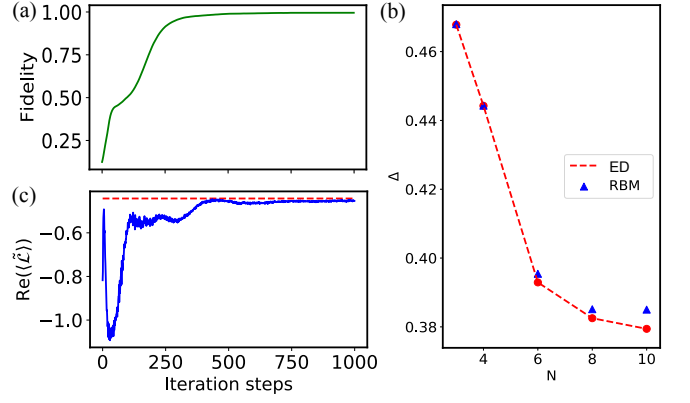


FIG. 3. Numerical results for the dissipative XYZ model in 1D. (a) and (b) show respectively the fidelity between  $|\rho'\rangle$  and  $|\rho_1\rangle$ , and the expectation value  $\text{Re}(\langle \tilde{\mathcal{L}} \rangle)$ , as functions of the iteration steps for  $N = 4$ . After around 500 iterations,  $\text{Re}(\langle \tilde{\mathcal{L}} \rangle)$  converges to the exact value of the Liouvillian gap  $\Delta$  [indicated by the red dashed line in (b)] with relative error  $\epsilon_{\text{rel}} \approx 10^{-2}$  and the fidelity approaches unit ( $|\langle \rho' | \rho_1 \rangle| \approx 0.991$ ). (c) The comparison between the RBM and ED results with varying system sizes. Here, the model parameters are chosen as  $J_x = 4$ ,  $J_y = 0.5$ ,  $J_z = 2$ , and  $\gamma = 1$ . All the ancillary  $\rho'_0$  used here are the identity matrices. More details on these numerical results are shown in the Supplemental Material [45].

gap corresponds to a single-magnon excitation, which leads to  $\Delta = \frac{\gamma}{2}$ , independent of  $J$ ,  $J_z$ , system size, and lattice geometry. In 1D with periodic boundary condition, the whole Liouvillian spectrum can be deduced from the Bethe ansatz solution [45]:

$$E(\{k_j\}_m) = -\frac{\gamma}{2}m \pm i \sum_{j=1}^m (2J \cos k_j - J_z). \quad (11)$$

Here the quasi-momentum of magnons  $\{k_j\}_m$  can be obtained by solving the Bethe equations:

$$e^{ik_j N} = \prod_{l \neq j} - \frac{J(e^{i(k_j+k_l)} + 1) - J_z e^{ik_j}}{J(e^{i(k_j+k_l)} + 1) - J_z e^{ik_l}}, \quad (12)$$

and the plus (minus) sign before the imaginary part represents the spectrum for the left (right) system.

We now turn to the anisotropic case with  $J_x \neq J_y$ , where the Liouvillian gap cannot be solved analytically in general. Our numerical results are shown in Fig. 3. From this figure, it is clear that our RBM results match the exact results from exact diagonalization within a reasonable accuracy. We note that, in Fig. 3(c), the apparent deviation of the RBM result for  $N = 10$  from its exact value is due to the small plotting range. A closer examination shows that for this point, the relative error is  $\epsilon_{\text{rel}} = 1.46 \times 10^{-2}$  in fact. In comparison with the case of the XXZ model, we find that the convergence for the XYZ model is notably slower. The reason for this is that for the XXZ model, its multiple first decay modes are orthogonal to each other. Hence, to obtain  $\Delta$ ,  $\rho'$  only needs to converge to a subspace spanned by these modes. Whereas for the XYZ

model, depending on the parameters there exist either only one or multiple but non-orthogonal first decay modes. Thus, as discussed previously in this case to obtain  $\Delta$  accurately,  $\rho'$  needs to converge to a single decay mode, which demands extra iteration steps and possibly more hidden neurons to increase the representation power [45].

*Discussion and conclusion.*—It is worthwhile to clarify that our RBM approach *cannot* solve the Liouvillian gap for all possible Liouvillian superoperators. In fact, no algorithm is capable of doing this due to the undecidability of the problem. Finding out the key properties of the Liouvillian superoperators that warrant the effectiveness of the RBM approach is of both fundamental and practical importance. Yet, this may require new physical concepts and a deeper understanding of artificial neural networks, similar to the case of how we understand the effectiveness of the density-matrix-renormalization-group algorithm [53] from the entanglement perspective. In addition, one may also use other neural networks, such as deep Boltzmann machine [54] or feedforward neural networks [39], to compute the the Liouvillian gap. More recently, a quantum-classical hybrid algorithm based on deep quantum neural networks has also been introduced to solve the steady states and dynamics for open systems [55]. It would also be interesting to extend this approach to compute the Liouvillian gap through noisy intermediate-scale quantum devices [56].

In summary, we have introduced a machine learning based approach to compute the Liouvillian gap for open quantum systems, which is generally applicable to high dimensional systems with massive entanglement. The accuracy and effectiveness of this approach have been benchmarked with numerical examples for the dissipative Heisenberg model in both one and two dimensions. Based on the numerical results, we found that the Liouvillian gap is exactly solvable for the dissipative XXZ model regardless of the system size and lattice geometry. These analytic results are of independent interest as well and may inspire subsequent analytical studies on open quantum systems.

We acknowledge helpful discussions with Fei Song and computational resources provided by Yiyang Wu and Benda Xu. Part of this project was completed during D.Y.'s visit to UC Berkeley, supported by Tsinghua Xuetang Cultivation Program. This work was supported by the start-up fund from Tsinghua University (Grant No. 53330300320) and NSFC under Grant No. 11674189.

---

\* These authors contributed equally to this work.

† [wangzhongemail@gmail.com](mailto:wangzhongemail@gmail.com)

‡ [dldeng@tsinghua.edu.cn](mailto:dldeng@tsinghua.edu.cn)

- [1] H.-P. Breuer and F. Petruccione, *The theory of open quantum systems* (Oxford University Press, Oxford, 2007).
- [2] D. A. Lidar, "Lecture notes on the theory of open quantum systems," [arXiv:1902.00967](https://arxiv.org/abs/1902.00967) (2019).
- [3] C. Noh and D. G. Angelakis, "Quantum simulations and many-body physics with light," *Rep. Prog. in Phys.* **80**, 016401 (2016).
- [4] M. A. Nielsen and I. L. Chuang, *Quantum computation and quantum information* (Cambridge university press, 2010).
- [5] M. V. Medvedeva, F. H. L. Essler, and T. c. v. Prosen, "Exact bethe ansatz spectrum of a tight-binding chain with dephasing noise," *Phys. Rev. Lett.* **117**, 137202 (2016).
- [6] T. Prosen, "Third quantization: a general method to solve master equations for quadratic open fermi systems," *New Journal of Physics* **10**, 043026 (2008).
- [7] L. Banchi, D. Burgarth, and M. J. Kastoryano, "Driven quantum dynamics: Will it blend?" *Phys. Rev. X* **7**, 041015 (2017).
- [8] D. A. Rowlands and A. Lamacraft, "Noisy spins and the richardson-gaudin model," *Phys. Rev. Lett.* **120**, 090401 (2018).
- [9] P. Ribeiro and T. c. v. Prosen, "Integrable quantum dynamics of open collective spin models," *Phys. Rev. Lett.* **122**, 010401 (2019).
- [10] N. Shibata and H. Katsura, "Dissipative spin chain as a non-hermitian kitaev ladder," *Phys. Rev. B* **99**, 174303 (2019).
- [11] N. Shibata and H. Katsura, "Dissipative quantum ising chain as a non-hermitian ashkin-teller model," *Phys. Rev. B* **99**, 224432 (2019).
- [12] A. A. Ziolkowska and F. H. Essler, "Yang-baxter integrable lindblad equations," *SciPost Physics* **8**, 044 (2020).
- [13] M. Nakagawa, N. Kawakami, and M. Ueda, "Exact liouvillian spectrum of a one-dimensional dissipative hubbard model," [arXiv:2003.14202](https://arxiv.org/abs/2003.14202) (2020).
- [14] S. Lloyd, "Quantum-mechanical computers and uncomputability," *Phys. Rev. Lett.* **71**, 943 (1993).
- [15] T. S. Cubitt, D. Perez-Garcia, and M. M. Wolf, "Undecidability of the spectral gap," *Nature* **528**, 207 (2015).
- [16] J. Bausch, T. Cubitt, A. Lucia, and D. Perez-Garcia, "Undecidability of the spectral gap in one dimension," [arXiv:1810.01858](https://arxiv.org/abs/1810.01858) (2018).
- [17] F. Verstraete, J. J. García-Ripoll, and J. I. Cirac, "Matrix product density operators: Simulation of finite-temperature and dissipative systems," *Phys. Rev. Lett.* **93**, 207204 (2004).
- [18] M. Zwolak and G. Vidal, "Mixed-state dynamics in one-dimensional quantum lattice systems: A time-dependent superoperator renormalization algorithm," *Phys. Rev. Lett.* **93**, 207205 (2004).
- [19] E. Mascarenhas, H. Flayac, and V. Savona, "Matrix-product-operator approach to the nonequilibrium steady state of driven-dissipative quantum arrays," *Phys. Rev. A* **92**, 022116 (2015).
- [20] J. Cui, J. I. Cirac, and M. C. Bañuls, "Variational matrix product operators for the steady state of dissipative quantum systems," *Phys. Rev. Lett.* **114**, 220601 (2015).
- [21] A. H. Werner, D. Jaschke, P. Silvi, M. Kliesch, T. Calarco, J. Eisert, and S. Montangero, "Positive tensor network approach for simulating open quantum many-body systems," *Phys. Rev. Lett.* **116**, 237201 (2016).
- [22] A. A. Gangat, T. I., and Y.-J. Kao, "Steady states of infinite-size dissipative quantum chains via imaginary time evolution," *Phys. Rev. Lett.* **119**, 010501 (2017).
- [23] A. Kshetrimayum, H. Weimer, and R. Orús, "A simple tensor network algorithm for two-dimensional steady states," *Nature communications* **8**, 1 (2017).
- [24] S. Finazzi, A. Le Boité, F. Storme, A. Baksic, and C. Ciuti, "Corner-space renormalization method for driven-dissipative two-dimensional correlated systems," *Phys. Rev. Lett.* **115**, 080604 (2015).
- [25] R. Rota, F. Minganti, C. Ciuti, and V. Savona, "Quantum critical regime in a quadratically driven nonlinear photonic lattice," *Phys. Rev. Lett.* **122**, 110405 (2019).
- [26] J. Jin, A. Biella, O. Viyuela, L. Mazza, J. Keeling, R. Fazio,

- and D. Rossini, “Cluster mean-field approach to the steady-state phase diagram of dissipative spin systems,” *Phys. Rev. X* **6**, 031011 (2016).
- [27] A. Nagy and V. Savona, “Driven-dissipative quantum monte carlo method for open quantum systems,” *Phys. Rev. A* **97**, 052129 (2018).
- [28] Z. Yan, L. Pollet, J. Lou, X. Wang, Y. Chen, and Z. Cai, “Interacting lattice systems with quantum dissipation: A quantum monte carlo study,” *Phys. Rev. B* **97**, 035148 (2018).
- [29] W. Casteels, R. M. Wilson, and M. Wouters, “Gutzwiller monte carlo approach for a critical dissipative spin model,” *Phys. Rev. A* **97**, 062107 (2018).
- [30] I. Goodfellow, Y. Bengio, and A. Courville, *Deep learning* (MIT press, 2016).
- [31] M. J. Hartmann and G. Carleo, “Neural-network approach to dissipative quantum many-body dynamics,” *Phys. Rev. Lett.* **122**, 250502 (2019).
- [32] F. Vicentini, A. Biella, N. Regnault, and C. Ciuti, “Variational neural-network ansatz for steady states in open quantum systems,” *Phys. Rev. Lett.* **122**, 250503 (2019).
- [33] A. Nagy and V. Savona, “Variational quantum monte carlo method with a neural-network ansatz for open quantum systems,” *Phys. Rev. Lett.* **122**, 250501 (2019).
- [34] N. Yoshioka and R. Hamazaki, “Constructing neural stationary states for open quantum many-body systems,” *Phys. Rev. B* **99**, 214306 (2019).
- [35] G. Carleo and M. Troyer, “Solving the quantum many-body problem with artificial neural networks,” *Science* **355**, 602 (2017).
- [36] G. Torlai and R. G. Melko, “Latent space purification via neural density operators,” *Phys. Rev. Lett.* **120**, 240503 (2018).
- [37] J. Carrasquilla, G. Torlai, R. G. Melko, and L. Aolita, “Reconstructing quantum states with generative models,” *Nature Machine Intelligence* **1**, 155 (2019).
- [38] L. Bianchi, E. Grant, A. Rocchetto, and S. Severini, “Modelling non-markovian quantum processes with recurrent neural networks,” *New Journal of Physics* **20**, 123030 (2018).
- [39] Z. Cai and J. Liu, “Approximating quantum many-body wave functions using artificial neural networks,” *Phys. Rev. B* **97**, 035116 (2018).
- [40] S. Sorella, M. Casula, and D. Rocca, “Weak binding between two aromatic rings: Feeling the van der waals attraction by quantum monte carlo methods,” *J. Chem. Phys.* **127**, 014105 (2007).
- [41] D.-L. Deng, X. Li, and S. Das Sarma, “Quantum entanglement in neural network states,” *Phys. Rev. X* **7**, 021021 (2017).
- [42] E. M. Kessler, G. Giedke, A. Imamoglu, S. F. Yelin, M. D. Lukin, and J. I. Cirac, “Dissipative phase transition in a central spin system,” *Phys. Rev. A* **86**, 012116 (2012).
- [43] F. Minganti, A. Biella, N. Bartolo, and C. Ciuti, “Spectral theory of liouvillians for dissipative phase transitions,” *Phys. Rev. A* **98**, 042118 (2018).
- [44] F. Song, S. Yao, and Z. Wang, “Non-hermitian skin effect and chiral damping in open quantum systems,” *Phys. Rev. Lett.* **123**, 170401 (2019).
- [45] See Supplemental Material at [URL will be inserted by publisher] for details on the stochastic reconfiguration, the analytical solution of the full Liouvillian spectrum for the dissipative XXZ model, and for more numerical data.
- [46] T. Viejira, C. Casert, J. Nys, W. De Neve, J. Haegeman, J. Ryckebusch, and F. Verstraete, “Restricted boltzmann machines for quantum states with non-abelian or anyonic symmetries,” *Phys. Rev. Lett.* **124**, 097201 (2020).
- [47] K. Choo, G. Carleo, N. Regnault, and T. Neupert, “Symmetries and many-body excitations with neural-network quantum states,” *Phys. Rev. Lett.* **121**, 167204 (2018).
- [48] T. E. Lee, S. Gopalakrishnan, and M. D. Lukin, “Unconventional magnetism via optical pumping of interacting spin systems,” *Phys. Rev. Lett.* **110**, 257204 (2013).
- [49] R. Rota, F. Storme, N. Bartolo, R. Fazio, and C. Ciuti, “Critical behavior of dissipative two-dimensional spin lattices,” *Phys. Rev. B* **95**, 134431 (2017).
- [50] R. Rota, F. Minganti, A. Biella, and C. Ciuti, “Dynamical properties of dissipative xyz heisenberg lattices,” *New Journal of Physics* **20**, 045003 (2018).
- [51] D. Huybrechts and M. Wouters, “Cluster methods for the description of a driven-dissipative spin model,” *Phys. Rev. A* **99**, 043841 (2019).
- [52] J. M. Torres, “Closed-form solution of lindblad master equations without gain,” *Phys. Rev. A* **89**, 052133 (2014).
- [53] U. Schollwöck, “The density-matrix renormalization group,” *Rev. Mod. Phys.* **77**, 259 (2005).
- [54] X. Gao and L.-M. Duan, “Efficient representation of quantum many-body states with deep neural networks,” *Nat. Commu.* , 662 (2017).
- [55] Z. Liu, L. M. Duan, and D.-L. Deng, “Solving quantum master equations with deep quantum neural networks,” [arXiv:2008.05488](https://arxiv.org/abs/2008.05488) (2020).
- [56] J. Preskill, “Quantum computing in the NISQ era and beyond,” *Quantum* **2**, 79 (2018).
- [57] S. Sorella, M. Casula, and D. Rocca, “Weak binding between two aromatic rings: Feeling the van der waals attraction by quantum monte carlo methods,” *The Journal of chemical physics* **127**, 014105 (2007).
- [58] K. Choo, G. Carleo, N. Regnault, and T. Neupert, “Symmetries and many-body excitations with neural-network quantum states,” *Phys. Rev. Lett.* **121**, 167204 (2018).
- [59] N. Metropolis, A. W. Rosenbluth, M. N. Rosenbluth, A. H. Teller, and E. Teller, “Equation of state calculations by fast computing machines,” *The journal of chemical physics* **21**, 1087 (1953).
- [60] J. C. Yipeng Wang, Wen-Li Yang and K. Shi, *Off-Diagonal Bethe Ansatz for Exactly Solvable Models* (Springer, Berlin, Heidelberg, 2015).
- [61] T. E. Lee, S. Gopalakrishnan, and M. D. Lukin, “Unconventional magnetism via optical pumping of interacting spin systems,” *Phys. Rev. Lett.* **110**, 257204 (2013).
- [62] D. Huybrechts, F. Minganti, F. Nori, M. Wouters, and N. Shammah, “Validity of mean-field theory in a dissipative critical system: Liouvillian gap,  $\mathbb{P}T$ -symmetric antigap, and permutational symmetry in the XYZ model,” *Phys. Rev. B* **101**, 214302 (2020).

## Supplementary Material for: Solving the Liouvillian Gap with Artificial Neural Networks

### THE STOCHASTIC RECONFIGURATION ALGORITHM

As mentioned in the main text, we adopt the stochastic reconfiguration (SR) method [35, 57, 58] to generate the real time evolution of the ansatz density matrix  $\rho'$ . We note that for closed quantum systems, this kind of variational optimization can be achieved equivalently by the standard stochastic gradient descent (SGD) or imaginary time evolution (via SR). However, due to the non-Hermiticity of Liouvillian superoperator  $\mathcal{L}$ , the orthogonality of right eigenstates is lost. The extreme value of  $\text{Re}(\langle \mathcal{L} \rangle)$ , which is usually used as the cost function, generally will not correspond to the Liouvillian gap  $\Delta$ . The appearance of crossing terms like  $\langle \rho_i | \rho_j \rangle$  ( $\{\rho_i\}$ ) are right eigenstates of  $\mathcal{L}$ ,  $i \neq j$ ) will lead to the failure of the former method for open quantum systems. This property can be clearly observed from Fig. 2 of the main text, where during the converging process,  $\text{Re}(\langle \mathcal{L} \rangle)$  has once exceeded the value of  $-\Delta$ .

In the framework of SR, given a variational ansatz  $|\rho'(\{\alpha_k\})\rangle$ , where  $\{\alpha_k\}$  stand for the real-number variational parameters like  $\{a_j, b_j, c_k, W_{j,k}^{R(L)}\}$  in the RBM, we need to optimize  $\{\alpha_k\}$  such that the trial bi-base wavefunction will finally converge to the first decay modes. First we define the logarithmic derivative operator for each parameter as

$$O_k = \frac{1}{|\rho'(\{\alpha_k\})\rangle} \partial_k |\rho'(\{\alpha_k\})\rangle = \partial_k \ln |\rho'(\{\alpha_k\})\rangle. \quad (\text{S1})$$

Note that  $O_k$  is diagonal under computational bi-bases  $\{|x\rangle = |\sigma_{1,R}^z, \sigma_{2,R}^z, \dots, \sigma_{N,R}^z, \sigma_{1,L}^z, \sigma_{2,L}^z, \dots, \sigma_{N,L}^z\rangle\}$

$$\langle x' | O_k | x \rangle = \delta_{x'x} \partial_k \ln \langle x | \rho' \rangle. \quad (\text{S2})$$

Consider a small change  $\{\delta\alpha_k\}$  on the parameters with respect to the initial values  $\{\alpha_k^0\}$

$$\alpha_k = \alpha_k^0 + \delta\alpha_k. \quad (\text{S3})$$

The corresponding bi-base wavefunction will deviate from the original term  $|\rho^0\rangle$  by

$$|\rho'\rangle = |\rho^0\rangle + \sum_k \delta\alpha_k O_k |\rho^0\rangle. \quad (\text{S4})$$

The stochastic reconfiguration scheme proceeds by performing a series of infinitesimal real time evolution governed by the Liouvillian superoperator  $\mathcal{L}$ , which up to the first order of learning rate  $\epsilon$  is given by

$$|\rho'_{\text{e}(\text{xact})}\rangle = e^{\epsilon\mathcal{L}} |\rho^0\rangle \approx (1 + \epsilon\mathcal{L}) |\rho^0\rangle. \quad (\text{S5})$$

Now we want to find out the optimal updated parameters  $\{\alpha_k\}$  to maximize the overlap between  $|\rho'\rangle$  and  $|\rho'_e\rangle$ . According to the fidelity relationship

$$\langle \rho'_e | \rho' \rangle \langle \rho' | \rho'_e \rangle = \langle \rho'_e | \rho'_e \rangle \langle \rho' | \rho' \rangle, \quad (\text{S6})$$

after some algebraic operations and dropping high-order terms like  $\epsilon^2$  or  $\epsilon\delta\alpha\delta\alpha$ , we obtain the linear equation

$$\begin{aligned} & \sum_{k'} \left( \langle O_k^\dagger O_{k'} \rangle + \langle O_{k'}^\dagger O_k \rangle - \langle O_k^\dagger \rangle \langle O_{k'} \rangle - \langle O_{k'}^\dagger \rangle \langle O_k \rangle \right) \delta\alpha_{k'} \\ & = \epsilon \left( \langle \mathcal{L}^\dagger O_k \rangle + \langle O_k^\dagger \mathcal{L} \rangle - \langle \mathcal{L}^\dagger \rangle \langle O_k \rangle - \langle O_k^\dagger \rangle \langle \mathcal{L} \rangle \right) \end{aligned} \quad (\text{S7})$$

where  $\langle \cdot \rangle$  denotes the average on the state  $|\rho^0\rangle$ .

In short Eq. (S7) can be written as  $\sum_{k'} S_{kk'} \delta\alpha_{k'} = \epsilon F_k$ , where  $S$  and  $F$  is usually called the covariant matrix and force. Finally by solving this linear equation the updated parameter vector can be computed as  $\delta\alpha = \epsilon S^{-1} F$ . Usually a regularization on  $S$  [35, 58] will be applied to decrease the fluctuation error generated in the Monte Carlo process that will be discussed in the next section:

$$\tilde{S} = S + \lambda I \quad \lambda \in [10^{-4}, 10^{-2}]. \quad (\text{S8})$$

We continuously repeat the iteration above to update the parameters until convergence.

Besides, for the case (iii) of first decay modes mentioned in the main text, in order to make the RBM ansatz further converge to the first decay mode with the minimal imaginary part, we should add another imaginary time evolution for  $\rho'$  under  $i\mathcal{L}$  with smaller learning rate  $\beta\epsilon$ . Hence, another force  $F'$  will be added

$$F'_k = -i\langle \mathcal{L}^\dagger O_k \rangle + i\langle O_k^\dagger \mathcal{L} \rangle + i\langle \mathcal{L}^\dagger \rangle \langle O_k \rangle - i\langle O_k^\dagger \rangle \langle \mathcal{L} \rangle, \quad (\text{S9})$$

and the linear equation becomes

$$\sum_{k'} S_{kk'} \delta\alpha_{k'} = \epsilon(F_k + \beta F'_k) \quad \beta \in [10^{-3}, 10^{-2}]. \quad (\text{S10})$$

Under the joint evolution of  $\mathcal{L} + i\beta\mathcal{L}$ ,

$$\begin{aligned} \rho' &= e^{(\mathcal{L} + i\beta\mathcal{L})t} \rho'^0 \\ &= c_0 \rho_0 + \sum_{i \neq 0} c_i e^{(\lambda_i + i\beta\lambda_i)t} \rho_i \quad (c_0 = 0) \\ &= \sum_{i \neq 0} c_i e^{(\text{Re}(\lambda_i) - \beta \text{Im}(\lambda_i))t} e^{i(\text{Im}(\lambda_i) + \beta \text{Re}(\lambda_i))t} \rho_i, \end{aligned} \quad (\text{S11})$$

where  $\rho_0$  denotes the steady state and  $\{\rho_i\}_{i \neq 0}$  are other decay eigenmodes. After long enough time, clearly  $\rho'$  will converge to the first decay mode with the minimal imaginary part. A numerical example belonging to this case will be shown in the last section.

### THE MARKOV CHAIN MONTE CARLO

In order to efficiently compute the average of observables mentioned in the previous section, we introduce the standard Markov chain Monte Carlo (MCMC) method as follows. Given an observable  $\hat{B}$  (like  $O_k$  and  $\mathcal{L}$ ), we convert its average into the stochastic form:

$$\begin{aligned} \langle \hat{B} \rangle &= \frac{\langle \rho' | \hat{B} | \rho' \rangle}{\langle \rho' | \rho' \rangle} \\ &= \sum_{x, x'} \frac{\langle \rho' | x \rangle \langle x | \hat{B} | x' \rangle \langle x' | \rho' \rangle}{\langle \rho' | \rho' \rangle} \\ &= \sum_{x, x'} \frac{\langle \rho' | x \rangle \langle x | \rho' \rangle}{\langle \rho' | \rho' \rangle} \frac{\langle x | \hat{B} | x' \rangle \langle x' | \rho' \rangle}{\langle x | \rho' \rangle} \\ &= \mathbb{E} \left( \sum_{x'} \frac{\langle x | \hat{B} | x' \rangle \langle x' | \rho' \rangle}{\langle x | \rho' \rangle} \right) \quad \text{by sampling } |\rho'|^2. \end{aligned} \quad (\text{S12})$$

Since  $O_k$  is diagonal under computational bi-bases, the explicit expressions of  $O_k$  for the RBM ansatz can be directly read out as follows:

$$O_{\text{Re}(a_j)} = \sigma_{j,R}^z \quad O_{\text{Im}(a_j)} = i\sigma_{j,R}^z \quad O_{\text{Re}(b_j)} = \sigma_{j,L}^z \quad O_{\text{Im}(b_j)} = i\sigma_{j,L}^z, \quad (\text{S13})$$

$$O_{\text{Re}(c_k)} = \tanh X_k \quad O_{\text{Im}(c_k)} = i \tanh X_k, \quad (\text{S14})$$

$$O_{\text{Re}(W_{k,j}^{R(L)})} = \sigma_{j,R(L)}^z \tanh X_k \quad O_{\text{Im}(W_{k,j}^{R(L)})} = i\sigma_{j,R(L)}^z \tanh X_k. \quad (\text{S15})$$

For achieving the stochastic average, we will generate a Markov chain of computational bi-bases  $x_1 \rightarrow x_2 \rightarrow x_3 \rightarrow \dots \rightarrow x_{N_s}$  with total length  $N_s$  by sampling  $|\rho'|^2$ . This process can be realized by the well-known Metropolis-Hasting algorithm [59]: At step  $i$ , we randomly flip 1 to 4 spins in  $x_i$  to obtain a new sample and calculate the following acceptance probability to determine whether to accept it:

$$A(x_i \rightarrow x_{i+1}) = \min \left( 1, \left| \frac{\rho_{x_{i+1}}}{\rho_{x_i}} \right|^2 \right). \quad (\text{S16})$$



Then we use the ensemble observable average of the Markov chain to estimate the stochastic average. Besides, we need to drop the first 5% of the Markov chain considering the thermalization process.

After each SR iteration, we should recompute the trace of updated RBM ansatz  $\rho_{\text{RBM}}$  in order to make sure  $\text{Tr}(\rho') = 0$ , as mentioned in the main text. This step can also be implemented in a sampling paradigm as follows.

$$\begin{aligned} \text{Tr}(\rho_{\text{RBM}}) &= \langle I | \rho_{\text{RBM}} \rangle \quad (|I\rangle = \sum_{l=1}^{2^N} |l, l\rangle) \\ &= 2^N \times \mathbb{E}(\rho_{\text{RBM}_{l,l}}) \\ &\text{by sampling a uniform distribution on } l \ (l = 1, \dots, 2^N) \end{aligned} \quad (\text{S17})$$

In our numerical calculations, the typical sampling size  $N_s$  is 2 to 5 times as many as the variational parameters. The ratio between hidden neurons and visible neurons  $M/2N$  is around 3 to 6. The learning rate is given by  $\epsilon = \max(0.01, 0.1 \times 0.96^p)$ ,  $\beta = 0.005 \sim 0.05$  ( $p$  is the iteration step). The regularization parameter takes  $\lambda = \max(10^{-4}, 0.9^p)$ . In summary, the total computational complexity for each SR iteration is bounded by the MCMC sampling and the matrix inversion operation, which both give the result  $O(N_{\text{par}}^3)$  ( $N_{\text{par}}$  is the number of variational parameters).

### EIGENSTATES OF THE DISSIPATIVE XXZ MODEL

As mentioned in the main text, the Liouvillian spectrum of dissipative XXZ model coincides with that of  $\tilde{\mathcal{L}}' = H_R + H_L$ , but not for the eigenstates. In this section we will give the general conditions for this kind of coincidence, and demonstrate how to construct the eigenstates of  $\mathcal{L}$  from that of  $\tilde{\mathcal{L}}'$  by following calculations in [52].

A Liouvillian superoperator  $\mathcal{L}$ , in the representation of Choi-Jamiołkowski isomorphism [18, 23] can always be decomposed into three parts:

$$\tilde{\mathcal{L}} = (-iH - \sum_{\mu} L_{\mu}^{\dagger} L_{\mu}) \otimes I + I \otimes (iH^T - \sum_{\mu} L_{\mu}^T L_{\mu}^*) + \sum_{\mu} 2L_{\mu} \otimes L_{\mu}^* = H_{\text{NH}} \otimes I + I \otimes H_{\text{NH}}^* + \sum_{\mu} D_{\mu}, \quad (\text{S18})$$

where  $H_{\text{NH}} = -iH - \sum_{\mu} L_{\mu}^{\dagger} L_{\mu}$  is the effective non-Hermitian Hamiltonian which governs the short-time coherent dynamics, and  $D_{\mu} = 2L_{\mu} \otimes L_{\mu}^*$  is the decoherence term for the quantum jump channel  $\mu$ . Consider the case when spectrum of  $H_{\text{NH}}$  can be solved exactly, which is easier than the whole Liouvillian spectrum in general since the dimension is reduced from  $2^{2N}$  to  $2^N$ , and there exists a conserved physical quantity  $M$  which commutes with the effective Hamiltonian:

$$[M, H_{\text{NH}}] = 0. \quad (\text{S19})$$

Meanwhile  $L_{\mu}$  is the lowering operator of  $M$ :

$$[M, L_{\mu}] = -m_{\mu} L_{\mu} \quad (\text{S20})$$

with well-defined negative real number  $m_{\mu} < 0$ .

According to the assumptions, the simultaneous eigenstates of  $H_{\text{NH}}$  and  $M$  have been solved, and denoted by two indices  $|m, j\rangle$ :

$$H_{\text{NH}}|m, j\rangle = E_{m,j}|m, j\rangle, M|m, j\rangle = m|m, j\rangle. \quad (\text{S21})$$

The corresponding left eigenstates are  $|\overline{m}, j\rangle$  with  $H_{\text{NH}}^{\dagger}|\overline{m}, j\rangle = E_{m,j}^*|\overline{m}, j\rangle$ . For simplicity we assume  $m$  to be integers, the lowest value of  $m$  is zero, and  $m_{\mu} = 1$  for all channels  $\mu$ . Index  $j$  labels different eigenstates with the same  $m$ , so the range of  $j$  depends on  $m$ , denoted by  $d_m$  in the following text. The effect of  $L_{\mu}$  is to lower  $m$  by 1:

$$L_{\mu}|m, j\rangle = \sum_k^{d_{m-1}} l_{\mu,jk}^{(m)} |m-1, k\rangle, \quad (\text{S22})$$

here  $l_{\mu,jk}^{(m)} = \langle \overline{m-1}, k | L_{\mu} | m, j \rangle$ .

For the coherent part of Liouvillian superoperator  $\tilde{\mathcal{L}}' = H_{\text{NH}} \otimes I + I \otimes H_{\text{NH}}^*$ , we can construct its eigenstates by the direct product:

$$\tilde{\mathcal{L}}'|m, j\rangle \otimes |n, k^*\rangle = (E_{m,j} + E_{n,k}^*)|m, j\rangle \otimes |n, k^*\rangle, \quad (\text{S23})$$

the superscript  $*$  on the state  $|n, k^*\rangle$  means the conjugation. Sort the eigenstates by  $m + n$  in increasing order, then due to the pure loss property of  $D_\mu$ ,

$$D_\mu |m, j\rangle \otimes |n, k^*\rangle = \sum_{j'}^{d_{m-1}} \sum_{k'}^{d_{n-1}} 2l_{\mu, j j'}^{(m)} l_{\mu, k k'}^{(n)*} |m-1, j'\rangle \otimes |n-1, k'^*\rangle. \quad (\text{S24})$$

The decoherent term takes an upper triangular form in this set of bases, so  $\tilde{\mathcal{L}}'$  and  $\mathcal{L}$  share the same spectrum.

As for the eigenstates of  $\mathcal{L}$ , the one with eigenvalue  $\lambda_{m, j; n, k} = E_{m, j} + E_{n, k}^*$  can be constructed as the linear superposition of  $|m, j\rangle \otimes |n, k^*\rangle$  together with all the other states having smaller  $m$  and  $n$ . For concreteness, given  $m \leq n$  the eigenstate can be expanded as

$$|m, j; n, k\rangle = |m, j\rangle \otimes |n, k^*\rangle + \sum_{r=1}^m \sum_{j'}^{d_{m-r}} \sum_{k'}^{d_{n-r}} C_{jk; j' k'}^{(mn), r} |m-r, j'\rangle \otimes |n-r, k'^*\rangle. \quad (\text{S25})$$

Then we solve the set of coefficients  $C_{jk; j' k'}^{(mn), r}$  by the eigenvalue equation

$$\tilde{\mathcal{L}} |m, j; n, k\rangle = \lambda_{m, j; n, k} |m, j; n, k\rangle. \quad (\text{S26})$$

It turns out that the equations are iterative, so that the algebraic relation from  $r-1$  to  $r$  is given by

$$C_{jk; j' k'}^{(mn), r} (\lambda_{m, j; n, k} - \lambda_{m-r, j'; n-r, k'}) = \sum_{j''}^{d_{m-r+1}} \sum_{k''}^{d_{n-r+1}} C_{jk; j'' k''}^{(mn), r-1} 2 \sum_{\mu} l_{\mu, j'' j'}^{(m-r+1)} l_{\mu, k'' k'}^{(n-r+1)*}. \quad (\text{S27})$$

For example, given  $C_{jk; j' k'}^{(mn), 0} = \delta_{j j'} \delta_{k k'}$ , from  $r=0$  to  $r=1$

$$C_{jk; j' k'}^{(mn), 1} = \frac{2}{\lambda_{m, j; n, k} - \lambda_{m-1, j'; n-1, k'}} \sum_{\mu} l_{\mu, j j'}^{(m)} l_{\mu, k k'}^{(n)*}. \quad (\text{S28})$$

When  $\lambda_{m, j' n, k} = \lambda_{m-1, j'; n-1, k'}$ , it implies that the Liouvillian superoperator is tuned to an exceptional point where both the eigenvalues and the corresponding eigenstates coincide, characterizing a unique feature of non-Hermitian matrices.

In the dissipative XXZ model, the right (left) single-magnon excitation  $|1, j\rangle \otimes |0\rangle$  ( $|0\rangle \otimes |1, j^*\rangle$ ), which decides the Liouvillian gap, has no matrix elements for  $D_\mu$  since  $l_{\mu, j k}^{(0)} = 0$ , so the first decay modes also coincide with single-magnon eigenstates of  $\tilde{\mathcal{L}}'$ .

## THE BETHE ANSATZ SOLUTION FOR THE EFFECTIVE HAMILTONIAN

In the main text we claim that the eigenspectrum of the Liouvillian superoperator  $\mathcal{L}$  for the dissipative XXZ model can be exactly obtained in 1D, by solving the effective non-Hermitian Hamiltonian. In this section we will demonstrate how to apply the Bethe ansatz on the effective Hamiltonian, for which eigenstates are magnon excitations over the reference state. Next we derive the Bethe equations to determine the quasi-momentum for two-magnon excitations and generalize the results to multi-magnon cases.

Take the right Hamiltonian in the main text

$$H_R = \sum_{i=1}^N [-iJ(S_{i,R}^+ S_{i+1,R}^- + S_{i,R}^- S_{i+1,R}^+) - iJ_z S_{i,R}^z S_{i+1,R}^z - \frac{\gamma}{2}(S_{i,R}^z + \frac{1}{2})]. \quad (\text{S29})$$

The periodic boundary condition is imposed by assuming  $S_{N+1} = S_1$ . The state with all  $S_{i,R}^z = -\frac{1}{2}$  is the eigenstate of  $H_R$  with eigenvalue  $E_g = -iJ_z \frac{N}{4}$ , and will be chosen as the reference state.

Following the well-known Bethe ansatz, the eigenstates are magnon excitations which mean spin flips from down to up, creating spin-one quasi-particles. Consider single-magnon excitations firstly:

$$|\Psi_1\rangle = \sum_{j=1}^N e^{ikj} |j\rangle, \quad (\text{S30})$$

where  $|j\rangle$  denotes the state with only the  $j^{\text{th}}$  spin being flipped up and others remaining down. To fulfill the boundary condition we need  $e^{ikN} = 1$  so that the quasi-momentum  $k$  can only take quantized values  $k = \frac{2\pi n}{N}$ ,  $n = 0, \dots, N-1$ . The eigenvalue of the state is  $E_k = -\frac{\gamma}{2} - i(2J\cos k - J_z) + E_g$ , whose real part gives the Liouvillian gap.

As for the two-magnon cases, considering the exchange of two magnons, the state is given by

$$|\Psi_2\rangle = \sum_{j_1 < j_2} (c_1 e^{i(k_1 j_1 + k_2 j_2)} + c_2 e^{i(k_1 j_2 + k_2 j_1)}) |j_1, j_2\rangle. \quad (\text{S31})$$

This is the eigenstate with eigenenergy  $E_{k_1, k_2} = -\gamma - i(2J\cos k_1 + 2J\cos k_2 - 2J_z) + E_g$  if and only if the two coefficients fulfill

$$\frac{c_1}{c_2} = -\frac{J(e^{i(k_1+k_2)} + 1) - J_z e^{ik_1}}{J(e^{i(k_1+k_2)} + 1) - J_z e^{ik_2}}. \quad (\text{S32})$$

Moreover, by imposing the boundary condition  $c_1/c_2 = e^{ik_1 N} = e^{-ik_2 N}$ , we obtain Bethe equations to determine the possible discrete values of quasi-momentum:

$$e^{ik_1 N} = e^{-ik_2 N} = -\frac{J(e^{i(k_1+k_2)} + 1) - J_z e^{ik_1}}{J(e^{i(k_1+k_2)} + 1) - J_z e^{ik_2}}. \quad (\text{S33})$$

The framework above can be generalized to the  $m$ -magnon wavefunction:

$$|\Psi_m\rangle = \sum_{j_1 < j_2 < \dots < j_m} \left[ \left( \sum_{\mathcal{P}} c_{\mathcal{P}} e^{i \sum_n^m k_{\mathcal{P}n} j_n} \right) |j_1, j_2, \dots, j_m\rangle \right], \quad (\text{S34})$$

where all possible permutations  $\mathcal{P}$  of integers  $1, \dots, m$  are taken into the summation. Now the eigenvalues are  $E(\{k_j\}_m) = -\frac{\gamma}{2}m - i \sum_{j=1}^m (2J\cos k_j - J_z) + E_g$ , while Bethe equations become

$$e^{ik_j N} = \prod_{l \neq j} -\frac{J(e^{i(k_j+k_l)} + 1) - J_z e^{ik_j}}{J(e^{i(k_j+k_l)} + 1) - J_z e^{ik_l}}. \quad (\text{S35})$$

For more details about Bethe ansatz, readers can refer to Ref. [60].

### THE MEAN-FIELD THEORY OF DISSIPATIVE XYZ MODEL

When the spin-spin interaction is anisotropic, the U(1) symmetry is broken, so that the Liouvillian spectrum is no longer exactly solvable. In this section we will apply a mean-field approximation to obtain the expectation value of physical quantities of the steady state, and identify the second-order phase transition, accompanied by the closing of Liouvillian gap. In one-dimensional system the mean-field theory fails due to strong quantum fluctuations, which are manifested by numerical results that the gap of one phase is much smaller than the other but never approaches zero.

To analyze the evolution of expectation value of operators, the adjoint Lindblad equation is needed:

$$\mathcal{L}^a(O) \equiv \frac{dO}{dt} = i[H, O] + \sum_{\mu} 2L_{\mu}^{\dagger} O L_{\mu} - \{L_{\mu}^{\dagger} L_{\mu}, O\}. \quad (\text{S36})$$

Analogous to its counterpart ‘‘Heisenberg picture’’ in closed quantum systems, the time-dependent operator is defined to preserve the expectation value in the original picture:

$$\text{Tr}(O(t)\rho(0)) = \text{Tr}(O\rho(t)). \quad (\text{S37})$$

With the adjoint Lindblad master equation, the evolution for local spin operators  $S_i^{\alpha}$ ,  $\alpha = x, y, z$  in the dissipative XYZ model are

$$\begin{aligned} \frac{dS_i^x}{dt} &= J_y(S_{i-1}^y + S_{i+1}^y)S_i^z - J_z(S_{i-1}^z + S_{i+1}^z)S_i^y - \frac{\gamma}{2}S_i^x, \\ \frac{dS_i^y}{dt} &= J_z(S_{i-1}^z + S_{i+1}^z)S_i^x - J_x(S_{i-1}^x + S_{i+1}^x)S_i^z - \frac{\gamma}{2}S_i^y, \\ \frac{dS_i^z}{dt} &= J_x(S_{i-1}^x + S_{i+1}^x)S_i^y - J_y(S_{i-1}^y + S_{i+1}^y)S_i^x - \gamma(S_i^z + \frac{1}{2}). \end{aligned} \quad (\text{S38})$$

Assuming the mean-field approximation which states that the many-body density matrix is the tensor product of identical density matrices for each site  $\rho = \otimes_{i=1}^N \rho_i$ , for every site  $i$ ,  $\text{Tr}(S_i^\alpha \rho) = \text{Tr}(S_i^\alpha \rho_i)$  is the same, defined as  $\langle S^\alpha \rangle$ . While for the operator product,

$$\text{Tr}(S_i^\alpha S_j^\beta \rho) = \text{Tr}(S_i^\alpha \rho_i) \text{Tr}(S_j^\beta \rho_j) = \langle S^\alpha \rangle \langle S^\beta \rangle, i \neq j. \quad (\text{S39})$$

Take the density matrix average of Eq. (S38). With the above approximation they are reduced to

$$\begin{aligned} \frac{d\langle S^x \rangle}{dt} &= 2(J_y - J_z) \langle S^y \rangle \langle S^z \rangle - \frac{\gamma}{2} \langle S^x \rangle, \\ \frac{d\langle S^y \rangle}{dt} &= 2(J_z - J_x) \langle S^z \rangle \langle S^x \rangle - \frac{\gamma}{2} \langle S^y \rangle, \\ \frac{d\langle S^z \rangle}{dt} &= 2(J_x - J_y) \langle S^x \rangle \langle S^y \rangle - \gamma \left( \langle S^z \rangle + \frac{1}{2} \right). \end{aligned} \quad (\text{S40})$$

For the steady state, we have the expectation value of  $S^z$ :

$$\langle S^z \rangle = -\frac{\gamma}{4\sqrt{(J_y - J_z)(J_z - J_x)}}. \quad (\text{S41})$$

The inequality relation  $|\langle S^z \rangle| \leq 1/2$  must be fulfilled on the steady state, which gives

$$\gamma^2 < 4(J_y - J_z)(J_z - J_x). \quad (\text{S42})$$

If so, the polarization on the steady state will deviate from  $z$ -direction so that  $\langle S^x \rangle, \langle S^y \rangle \neq 0$ . Moreover, since the parity operator  $P = \prod_{j=0}^{N-1} e^{i\pi(S_j^z + \frac{1}{2})}$  commutes with the Liouvillian superoperator, which reverses  $S^x$  and  $S^y$ , steady states must be at least two-fold degenerate and span a steady subspace as the eigenspace of  $P$ , implying the closing of Liouvillian gap. It is the counterpart of spontaneous symmetry breaking in quantum mechanics, though here the relations between symmetry and conservation laws are more sophisticated than unitary cases. On the other hand, when the parameters violate the inequality, the tensor product ansatz  $\rho = \otimes_{i=1}^N \rho_i$  will fail. The steady state polarization approaches the maximal value  $1/2$ , and the Liouvillian gap is opened between the unique steady state and the first decay modes. In Fig. 3 of the main text, the system with chosen parameters lies in the degenerate phase, though quantum fluctuations open the gap, while for higher dimensions [26, 61] or all-to-all connected lattices [62] the critical dynamics will occur.

## MORE NUMERICAL RESULTS AND DISCUSSIONS

In this section we will provide more numerical results and relevant discussions. In Fig. S1, we display the Liouvillian spectrum of 1D dissipative XYZ model with different parameters obtained by exact diagonalization (ED). The panel (a), (b), (c) respectively correspond to the XXZ case, gapped XYZ phase, and ‘‘gapless’’ XYZ phase (actually gapped due to strong quantum fluctuations in 1D). The latter two have been discussed in the previous section. As mentioned in the main text, in comparison with the XXZ case, the reason for the slower convergence of XYZ model is that: The XXZ model has multiple orthogonal first decay modes (both deduced from the third section and tested numerically), like the case (a), so that  $\rho'$  only needs to converge to a subspace spanned by these modes. Whereas for the XYZ model, there exists either only one or multiple but non-orthogonal first decay modes (tested numerically), like the case (b) and (c), such that in order to obtain the Liouvillian gap  $\Delta$  accurately,  $\rho'$  needs to converge to a single first decay mode, which demands extra iteration steps, longer Markov chains and more hidden neurons of the RBM.

For the panel (a) of Fig. S2, we show the precise convergence behaviour for Liouvillian gap computation of 1D dissipative XYZ model (‘‘gapless’’ phase) obtained by the RBM, corresponding to Fig. 3 of the main text. It can be observed that the differences between Liouvillian gap of  $N = 6, 8, 10$  are relatively small. The largest relative error is of order  $10^{-2}$ . The panel (b) shows an example of the gapped XYZ phase with multiple non-orthogonal first decay modes, where we need the joint evolution  $\mathcal{L} + i\beta\mathcal{L}$  mentioned in the first section. Due to the smaller learning rate  $\beta\epsilon$  on the imaginary part, we need to devote more numerical efforts. The violent oscillation of  $\text{Im}\langle \mathcal{L} \rangle$  before convergence is reasonable since the Liouvillian spectrum is symmetric with respect to the real axis.

Finally, in this paper, we mainly discuss the computation of Liouvillian gap for open quantum systems with only one steady state. In order to tackle the cases with multiple steady states by the RBM, the orthogonalization process should be more complicated due to the necessary introduction of left and right eigenstates, which will be left for future explorations.

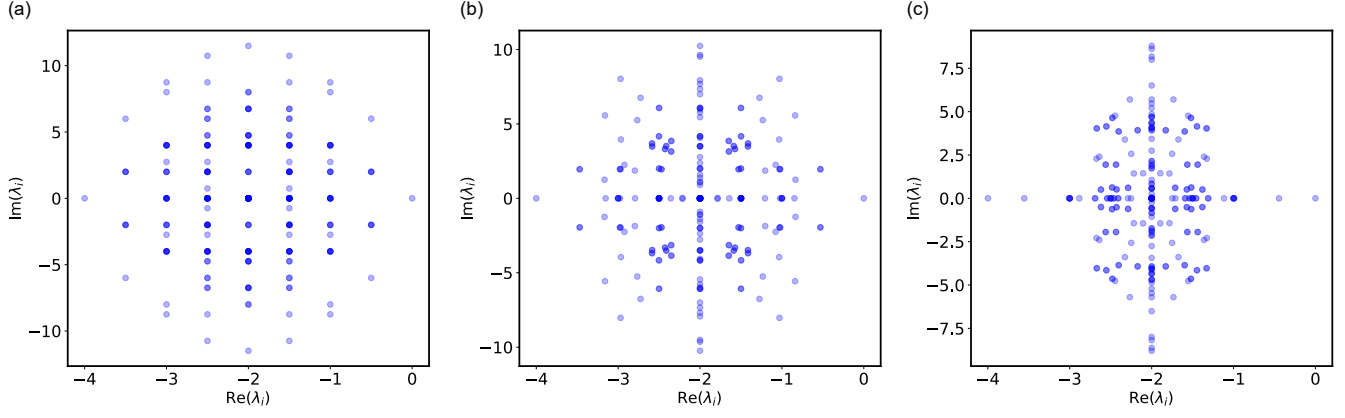


FIG. S1. The Liouvillian spectrum for the dissipative XYZ model in 1D, obtained by ED. The model parameters are chosen as  $N = 4$ ,  $\gamma = 1$ ,  $J_x = 4$ , and  $J_z = 2$ . (a)  $J_y = 4$ . The XXZ case with multiple orthogonal first decay modes. (b)  $J_y = 3$ . The gapped XYZ case with multiple non-orthogonal first decay modes. (c)  $J_y = 0.5$ . The “gapless” XYZ case with only one first decay mode. The color shade stands for the degeneracy of each eigenvalue  $\lambda_i$ .

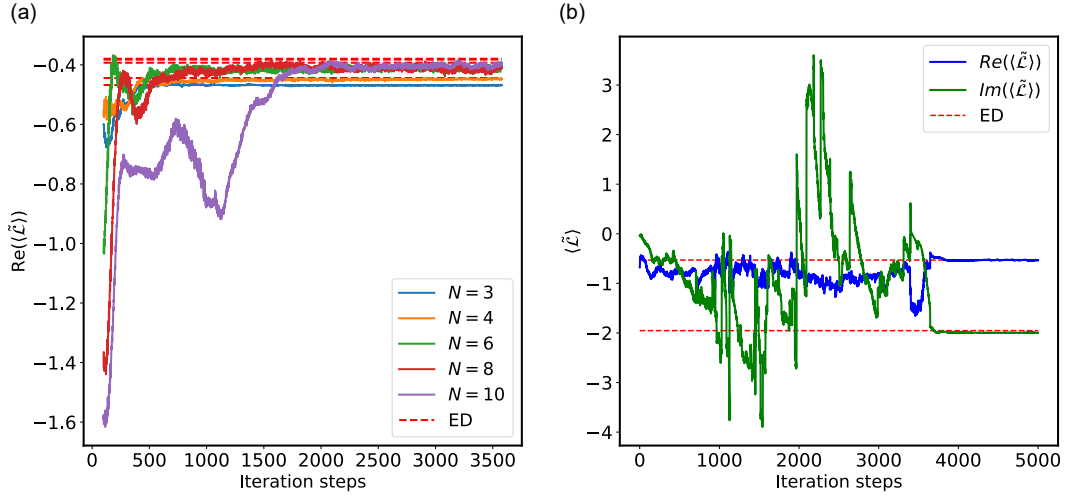


FIG. S2. Convergence behaviour for Liouvillian gap computation of 1D dissipative XYZ model, obtained by the RBM. (a)  $\text{Re}(\langle \tilde{\mathcal{L}} \rangle)$  as a function of the iteration steps for different lattice size  $N$ .  $J_x = 4$ ,  $J_y = 0.5$ ,  $J_z = 2$ , and  $\gamma = 1$ . The systems lie in the “gapless” XYZ phase with only one first decay mode. All the ancillary  $\rho'_0$  used here are the identity matrices. (b)  $\text{Re}(\langle \tilde{\mathcal{L}} \rangle)$  and  $\text{Im}(\langle \tilde{\mathcal{L}} \rangle)$  as a function of the iteration steps for the gapped XYZ phase.  $N = 4$ ,  $J_x = 4$ ,  $J_y = 3$ ,  $J_z = 2$  and  $\gamma = 1$ . There exist multiple non-orthogonal first decay modes so that we need the joint evolution  $\mathcal{L} + i\beta\mathcal{L}$  mentioned in the first section. The ancillary  $\rho'_0$  used here corresponds to the bi-base state with all spins pointing down.